Correlation Polarimeter for Millimeter-Wave Wavefront Sensing

Makoto Nagai, Hiroaki Imada, Tom Nitta, Yosuke Murayama, Ryohei Noji, and Masato Naruse

Abstract – The mirror surface measurement is of great importance for next-generation radio telescopes with a large single dish for millimeter- and submillimeter-wave astronomy. Wavefront sensing in millimeter wave is necessary to realize adaptive optics that can compensate for mirror deformation with short timescales. To measure the field distribution of a beam, we propose a new type of correlation polarimeter array based on phase-shifting interferometry. We are developing a correlation polarimeter that is easy to fabricate a large-format array. The polarimeter is implemented as a superconducting film on a silicon wafer, which uses a dual-polarization twin-slot antenna, a delay circuit composed of coplanar waveguide, and microwave kinetic inductance detectors (MKID). We developed a pixel design for 100 GHz, made electromagnetic simulations of the components, and are preparing for trial production.

1. Introduction

The mirror surface measurement to maintain the surface accuracy is of great importance for next-generation ground-based radio telescopes with a large single dish for millimeter- and submillimeter-wave astronomy, because the surface accuracy is directly related to the telescope performance. Though radio holography is used to measure the mirror surface, a faster method is necessary to realize adaptive optics that can compensate for unpredictable mirror deformation with short timescales. The main cause of such deformation is the wind load to the primary mirror whose timescale is typically 10^{-1} s to 1 s [1]. Real-time wavefront sensing in millimeter-wave can serve as a solution for this issue.

Unfortunately, wavefront sensors such as a Shack–Hartmann sensor used in the visible and near-infrared regime are not available for millimeter waves. Though millimeter-wave receivers can take phase information, a large-format receiver array involves a high cost. One proposed solution is aperture plane interferometry, which places a transmitter array on the primary mirror [1]. Another proposed way of wavefront sensing is the radio point diffraction interferometer (RPDI) [2], which is a point diffraction interferometer [3, 4] for radio bands. In the RPDI setup, the test beam is projected to a linear polarization, and a reference beam in the orthogonal polarization is generated with a point diffraction source. The interferograms between the test and reference beams with several phase differences are acquired by a kind of polarimeter camera. The amplitude and phase of the test beam can be calculated based on the phase-shifting interferometry [5]. Each pixel of an RPDI camera can be assembled with an orthomode transducer, a waveguide delay circuit, and power detectors. The detector with this function can be regarded as a kind of a correlation polarimeter [6, 7].

In this article, we propose a new type of correlation polarimeter that can be used as a pixel of a large-format array to measure the wavefront of a millimeter-wave beam using a setup similar to the RPDI. The new correlation polarimeter is developed using the technology of the Nobeyama MKID camera [8, 9]. The correlation polarimeter consists of a dual-polarization twin-slot antenna, a delay circuit composed of a coplanar waveguide (CPW), and microwave kinetic inductance detectors (MKID). It can be implemented as a single-layer superconducting film on a silicon wafer. In particular, a delay circuit with no interchange is possible with CPW 90° hybrid and 180° hybrid couplers. We developed a pixel design for 100 GHz. We made electromagnetic (EM) simulations of the components for test, and the desired characteristics are successfully obtained.

2. Concept of Correlation Polarimeter Array for Wavefront Sensing

The basic setup of wavefront sensing using a correlation polarimeter array is shown in Figure 1. To measure the distribution of a test beam of a certain polarization, a beam of the orthogonal polarization with known amplitude and phase distribution is prepared as a reference. Both signals of the test and reference beams are received by each pixel and go through the delay circuit. The signals are split into several paths and given

Manuscript received 28 December 2022. This work was supported by the Japan Society for the Promotion of Science (JSPS) Grants-in-Aid for Scientific Research (KAKENHI) Grant Number 19K03920.

Makoto Nagai, Hiroaki, Imada, and Yosuke Murayama are with the Advanced Technology Center, National Astronomical Observatory of Japan, 2-21-1 Osawa, Mitaka, Tokyo 181-8588, Japan; e-mail: makoto.nagai@nao.ac.jp.

Tom Nitta is with the Faculty of Pure and Applied Sciences, University of Tsukuba, 1-1-1 Tennnodai, Tsukuba, Ibaraki, 305-8577, Japan.

Ryohei Noji is with the Graduate School of Pure and Applied Sciences, University of Tsukuba, 1-1-1 Tennnodai, Tsukuba, Ibaraki, 305-8577, Japan.

Masato Naruse is with the Graduate School of Science and Engineering, Saitama University Shimo-Okubo 255, Sakura-ku, Saitama-shi, 338-8570, Japan; e-mail: naruse@super.ees.saitama-u.ac.jp.

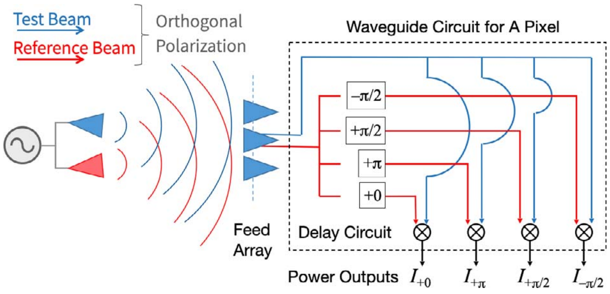

Figure 1. Wavefront sensing with correlation polarimeter array.

desired phase differences. The test and reference signals are coupled and detected by power detectors. As a result, their interferograms with various phase differences are simultaneously obtained. Because the test beam and the reference beam should be coherent, they are generated by the same oscillator in Figure 1. When the reference beam is generated by a point diffraction source from the test beam, the setup becomes the RPDI.

The interferogram outputs enable us to determine the amplitude and phase of the test beam based on the phase-shifting interferometry [5]. The output with phase difference θ can be written as

$$I_\theta = g|e^{\sqrt{-1}\theta} \cdot E_c + E_x|^2 \tag{1}$$

where E_c and E_x are the copolarization (test) and cross-polarization (reference) complex amplitude, respectively, and g is the gain. Standard values of the phase difference are four values with intervals of 90°, i.e., 0°, 90°, 180°, and 270°. The in-phase and quadrature components of the test signal for the reference signal, namely X and Y, respectively, are written as follows:

$$\begin{aligned} X &= (I_{0^\circ} - I_{180^\circ})/g \\ Y &= (I_{90^\circ} - I_{270^\circ})/g \end{aligned} \tag{2}$$

When the test beam is vertical polarization and the reference beam is horizontal polarization, this instrument is a correlation polarimeter that acquires the cross correlation of two linear polarizations. In this case, the relation of X and Y to Stokes parameters [10] becomes simple as

$$\begin{aligned} S_0 &= X_0^2 + |X|^2 + |Y|^2 \\ S_1 &= X_0^2 - |X|^2 - |Y|^2 \\ S_2 &= 2 \cdot X_{0_X} \\ S_3 &= 2 \cdot X_{0_Y} \end{aligned} \tag{3}$$

where X_0 is the amplitude of the horizontal polarization.

3. Implementation for Millimeter-Wave Band

We propose a new correlation polarimeter implemented with a superconducting circuit. Superconducting circuits can be low loss and low noise. The transmission lines are CPW on a silicon wafer, making the structure and fabrication simple. MKID can be used as power detectors that afford natural frequency domain multiplexing.

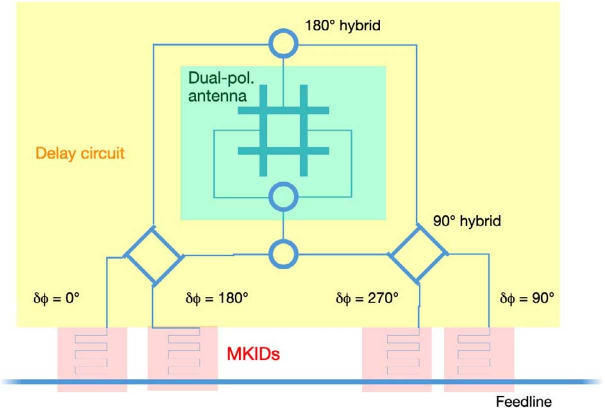

Figure 2. Schematic of a correlation polarimeter pixel.

In addition, our technology with the Nobeyama MKID camera for 100 GHz enables us to develop the correlation polarimeter array. The array will be fabricated on a 3 in. silicon wafer. Each polarimeter is coupled to telescope optics with cold camera optics and a silicon lenslet on the focal plane. The power detectors of the polarimeter are NbTiN and Al hybrid MKID [9]. MKID up to a few 10^2 can be read out through a single line with the readout system of the Nobeyama MKID camera [8]. Prototypes of a correlation polarimeter can be tested on the cryostat of the Nobeyama MKID camera with the same cold optics and the silicon lenslet array. There are items for development, not used in our camera: dual-polarization plane antenna, delay circuit, and the connection between the delay circuit and an MKID.

4. Pixel Design

A schematic of the correlation polarimeter pixel is shown in Figure 2. The incident beam focused by a lenslet is coupled to a dual-polarization plane antenna. We can use a double twin-slot antenna fed by CPW lines [11]. The antenna is scaled to 100 GHz, and the two CPW lines of the horizontal polarization are connected to an antiphase combiner. The two outputs of the dual-polarization plane antenna are led to a delay circuit. Figure 3 shows a schematic diagram of the delay circuit. In the delay circuit, the inputs are split into two

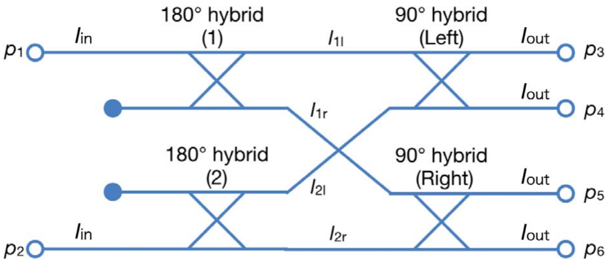

Figure 3. Schematic diagram of the delay circuit.

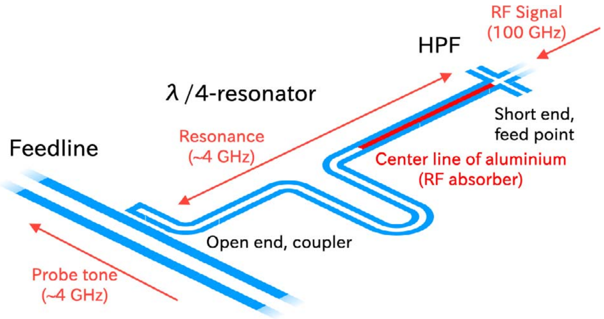

Figure 4. Schematic of power detector with an MKID.

by 180° hybrid couplers and coupled by 90° hybrid couplers. The lengths of the transmission lines are adjusted so that the phase differences become the desired values. We can take a condition $l_{1l} = l_{1r} = l_{2l} = l_{2r} - \pi/(4\beta)$, where β is the phase constant. Each output of the delay circuit is led to a power detector with an MKID, as shown in Figure 4. The signal is passed to the MKID through a high-pass filter (HPF) that becomes a short end at lower frequencies. The MKID is a CPW quarter-wavelength resonator whose center line has an aluminium section as an absorber for 100 GHz signals. The open end of the MKID is coupled to the feedline, where probe tones go through. The resonant frequencies of the MKID in the array are made different for frequency domain multiplexing.

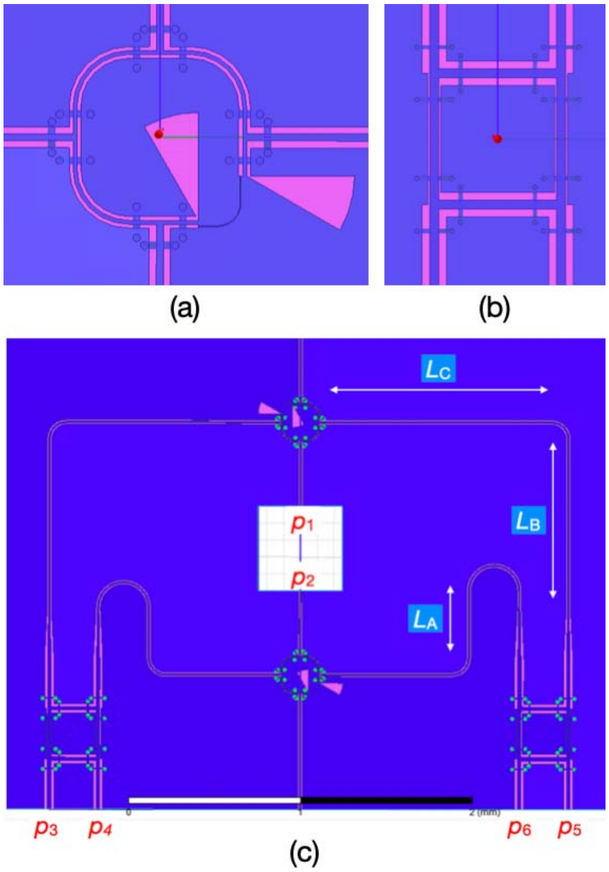

Figure 5. Simulation models: (a) rat-race coupler; (b) branch-line coupler; and (c) delay circuit.

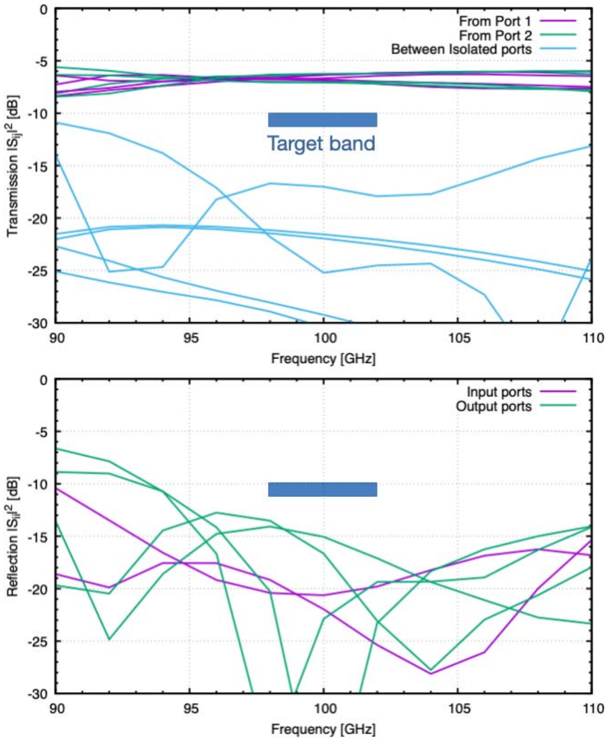

Figure 6. Simulation result of the delay circuit: (top) transmission; and (bottom) reflection.

5. EM Simulations of Circuit Components

We made a three-dimensional EM simulation of circuit components of the correlation polarimeter pixel using the HFSS software. Figure 5a shows a CPW rat-race coupler with a slotline phase inverter for 100 GHz. This coupler is used as the antiphase combiner in the plane antenna and a 3 dB power divider in the delay circuit. A CPW branch-line coupler for 100 GHz (Figure 5b) is used as a 90° hybrid coupler in the delay circuit. Figure 5c shows a test model of the whole delay circuit. The central region where the plane antenna is placed is made smaller than the actual size to reduce the calculation cost. The lengths L_A, L_B, and L_C can be adjusted to tune the output phase differences. The difference of length L_A in the left-hand and right-hand sides corresponds to the difference of l_{2l} and l_{2r}. In these models, the smallest line width is 1 μm, slightly larger than the processing accuracy.

The simulation results of the delay circuit are shown in Figure 6 and Figure 7. *S* paramters from input ports to output ports $|S_{ij}|^2$ in the target band (98 GHz to102 GHz) are just below –6 dB, and reflections $|S_{ii}|^2$ are below −13 dB. The phase intervals of port 1 signals are about ± 90°, while those of port 2 signals are about 90°. We checked the phase dependence on L_A, L_B, and

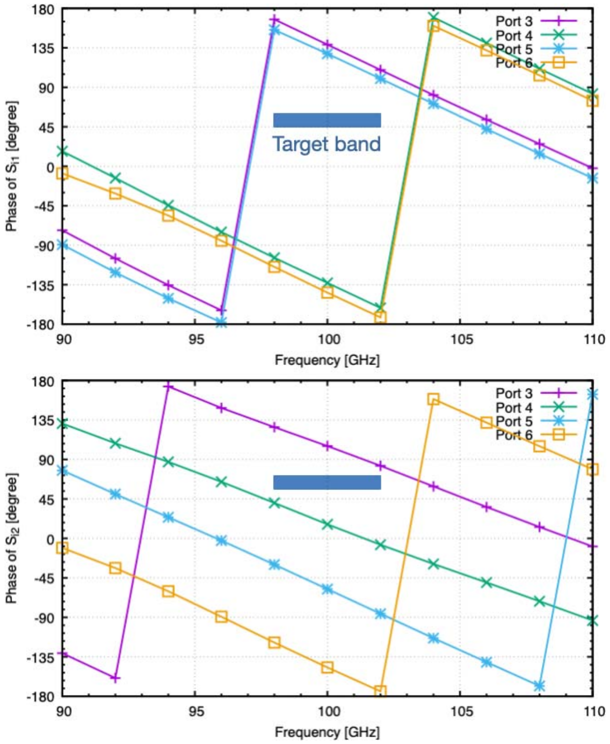

Figure 7. Simulation result of phase shift induced by the delay circuit: (top) from port 1; and (bottom) from port 2.

L_C and found that each output phase shifts, depending on the line lengths as expected. Thus, the delay circuit property for phase-shifting interferometry is obtained as desired. We also made simulations of a 100 GHz HPF and obtained good properties, insertion loss about 1 dB, and reflection below –25 dB at 100 GHz.

6. Conclusion

We are developing a correlation polarimeter for wavefront sensing that is easy to fabricate a large-format array using Nobeyama MKID camera technology. The polarimeter makes it possible to simultaneously obtain interferograms with four phase differences for phase-shifting interferometry. The polarimeter is implemented as a single-layer superconducting film on a silicon wafer. We developed a pixel design for 100 GHz and made EM simulations of the components. Desired circuit properties are successfully obtained.

We are preparing to fabricate a test pixel for verification. Development of a dual-polarization plane antenna with improved polarization characteristics will be a key point for the trial production of the correlation polarimeter.

7. References

1. Y. Tamura, R. Kawabe, Y. Fukasaku, K. Kimura, T. Ueda, et al., “Wavefront Sensor for Millimeter/Submillimeter-Wave Adaptive Optics Based on Aperture-Plane Interferometry,” *Society of Photo-Optical Instrumentation Engineers Conference Series*, **11445**, December 2020, p. 114451N.
2. T. Okumura, H. Imada, M. Nagai, T. Nitta, N. Nakai, et al., “Point-Diffraction Interferometer for Radio Telescopes,” *Society of Photo-Optical Instrumentation Engineers Conference Series*, **9906**, August 2016, p. 990641.
3. K. Yamamoto, T. Matsuo, H. Imada, and M. Kino, “Measurement of Complex Amplitude With a Point-Diffraction Interferometer,” *Applied Optics*, **54**, 26, September 2015, pp. 7895-7903.
4. H. Imada, T. Matsuo, K. Yamamoto, and M. Kino, “Real-Time Point-Diffraction Interferometer and Its Analytical Formulation,” *Applied Optics*, **54**, 26, September 2015, pp. 7870-7878.
5. H. Schreiber and J. H. Bruning, “Phase Shifting Interferometry,” in D. Malacara (ed.), *Optical Shop Testing*, New York, Wiley, 2007, Chapter 14.
6. C. Thum, H. Wiesemeyer, D. Morris, S. Navarro, and M. Torres, “Versatile IF Polarimeter at the IRAM 30m Telescope,” *Society of Photo-Optical Instrumentation Engineers Conference Series*, **4843**, February 2003, pp. 272-283.
7. C. Thum, H. Wiesemeyer, G. Paubert, S. Navarro, and D. Morris, “XPOL—the Correlation Polarimeter at the IRAM 30-m Telescope,” *Publications of the Astronomical Society of the Pacific*, **120**, 869, July 2008, p. 777.
8. M. Nagai, S. Hisamatsu, G. Zhai, T. Nitta, N. Nakai, et al., “Data Acquisition System of Nobeyama MKID Camera,” *Journal of Low Temperature Physics*, **193**, 3–4, November 2018, pp. 585-592.
9. Y. Murayama, “Development of 109-Pixel MKID Arrays for the 100-GHz Band Continuum Camera,” Ph.D. dissertation, University of Tsukuba, Japan, 2022.
10. E. Collett, *Field Guide to Polarization*, Bellingham, WA, SPIE, 2005.
11. M. Naruse, T. Nitta, K. Karatsu, M. Sekine, S. Sekiguchi, et al., “Dual-Double Slot Antennas Fabricated With Single Superconducting Film for Millimeter Wave Camera,” *Journal of Infrared*, **37**, 2, February 2016, pp. 128–136.